Chinese Journal of Mechanical Engineering

ORIGINAL ARTICLE

Open Access

Optimization Mechanism of Mechanical Properties of Basalt Fiber-Epoxy Resin Composites by Interfacially Enriched Distribution of Nano-Starch Crystals

Yanpeng Wei[1], Jiale Zhao[2]* , Jian Zhuang[1]*, Peng Zhang[3] and Zhiwu Han[2]

Abstract

Fibre reinforced polymer composites have become a new generation of structural materials due to their unique advantages such as high specific strength, designability, good dimensional stability and ease of large-area monolithic forming. However, the problem of interfacial bonding between the resin matrix and the fibres limits the direct use of reinforcing fibres and has become a central difficulty in the development of basalt fibre-epoxy composites. This paper proposes a solution for enhancing the strength of the fibre-resin interface using maize starch nanocrystals, which are highly yield and eco-friendly. Firstly, in this paper, corn starch nanocrystals (SNC) were prepared by hydrolysis, and were deposited on the surface of basalt fibers by electrostatic adsorption. After that, in order to maximize the modification effect of nano-starch crystals on the interface, the basalt fiber-epoxy resin composite samples were prepared by mixing in a pressureless molding method. The test results shown that the addition of basalt fibers alone led to a reduction in the strength of the sample. Deposition of 0.1 wt% SNC on the surface of basalt fibers can make the strength consistent with pure epoxy resin. When the adsorption amount of SNC reached 0.5 wt%, the tensile strength of the samples was 23.7% higher than that of pure epoxy resin. This is due to the formation of ether bond homopolymers between the SNC at the fibre-epoxy interface and the epoxy resin, which distorts the originally smooth interface, leading to increased stress concentration and the development of cracks. This enhances the binding of basalt fibers. The conclusions of this paper can provide an effective, simple, low-cost and non-polluting method of interfacial enhancement modification.

Keywords Basalt fibres, Epoxy resin, Fibre reinforced composites, Starch nanocrystals, Eco-friendly

*Correspondence:
Jiale Zhao
zhaojl@jlu.edu.cn
Jian Zhuang
zhuangjian_2001@163.com
[1] College of Biological and Agricultural Engineering, Jilin University, Changchun 130025, China
[2] Key Laboratory of Bionics Engineering, Ministry of Education, Jilin University, Changchun 130025, China
[3] Weichai Lovol Heavy Industry Co., LTD, Weifang 261031, China

1 Introduction

As an emerging green industrial material, basalt fiber-epoxy composites are widely used in many fields such as aviation, ships and automobiles [1]. Reinforced phase basalt fibres with the advantages of green and pollution-free, high mechanical strength, good temperature resistance and chemical stability [2–4]. Because of the good mechanical properties, resistance to moisture absorption, corrosion resistance, durability and versatility of the base epoxy resin, it is one of the most widely used thermosetting polymers in practical application [1]. Basalt fibre-epoxy composites are prepared by fusing together

Wei *et al. Chinese Journal of Mechanical Engineering*   (2024) 37:44

Page 2 of 8

the basalt fibres and epoxy resin. The composite has better mechanical properties than traditional glass fibre reinforced epoxy composites and is cheaper to manufacture than carbon fibre reinforced epoxy composites [5]. This makes basalt fibre-reinforced epoxy composites considered to be the most widely used fibre-reinforced composites of the future [6].

Poor interfacial bonding between basalt fibers and resin matrix is the main reason limiting the application and promotion of basalt fiber-epoxy resin composites [7, 8]. This is due to the inert surface of the basalt fibres and their high smoothness [9, 10]. These disadvantages make it difficult to introduce groups on the surface of basalt fibres that can bind to polymers and have poor wettability with epoxy resin substrates, fibres do not provide excellent mechanical load-bearing during service [11–13].

Current research into improving the interface bonding between fibres and matrix materials suffers from environmental pollution, reduced mechanical properties of composites, chemical corrosion. For instance, the modification of the resin matrix by the addition of silane coupling agents to the composite, oxidation of the fibre surface or addition of third phase nanoparticles [5, 14–17]. These methods require the use of highly corrosive and polluting chemical agents for surface activation, which will reduce the mechanical properties of the fibres, and the addition of nanoparticles can cause unknown harm to the environment [18–21]. Therefore, an effective and non-polluting method to improve the interfacial bonding of basalt fibers with resin matrix is urgently needed.

The starch nanocrystals, from maize starch may offer a new solution to the above core problems. Cellulose nanofibres (CNF) and cellulose nanocrystals (CNC), which are also polysaccharide nanocrystals, have been added to the epoxy resin composites as reinforcing phases to improve the mechanical properties of the composites [22–25]. SNC has been studied more in the field of lifting rubber and composite films, but less in the field of epoxy composites [26–28]. By introducing a small amount of starch nanocrystals (SNC) into basalt fibre-epoxy composites, particularly at the basalt fibre-epoxy interface, this study aims to determine whether SNC can improve the mechanical properties of the composite, alter the interfacial bonding and elucidate the underlying mechanism of its effect. Such an approach could provide an environmentally friendly solution to the fundamental challenges faced by basalt fibre-epoxy composites, while expanding the use of natural polymers such as SNC in epoxy resin-based composites.

In this paper, we are aimed at the need to improve the interface bonding between basalt fibres and resin matrix, and based on the great potential of maize industrial treatment products in this field, we investigate the modification of the basalt fibre-resin matrix interface using starch nanocrystals (SNC), a natural polymer extracted from maize starch. In order to comprehensively demonstrate the reinforcing principle of the widely available natural polymer, starch nanocrystals (SNC), at the fibre-resin interface, the experiment used the most intuitive and non-reinforcing method of sample preparation, the pressureless moulding technique. The resulting specimens were then subjected to mechanical tensile tests. After the tests, the morphology of the specimens was characterised. The mechanism of the reinforcing effect of starch nanocrystals on the interface between the basalt fibre and the resin matrix was analysed.

## 2 Materials and Methods
2.1 Materials
The resin matrix category chosen for this study is bisphenol A. epoxy resin (Wuxi Xinyehao Chemical Co., Ltd., GM-128, density 1.15 g/cm^3). The selected reinforcing fibre is basalt fibre (Jilin Tongxin Basalt Co., Ltd., length 7±0.3 mm, diameter 12±0.3 μm). Starch nanocrystals (SNC) were produced from maize starch by sulphuric acid digestion hydrolysis and the crystallinity of the starch granules obtained after 6 days of acid digestion was 64.7%.

2.2 Preparation of SNC
Starch nanocrystals prepared by sulphuric acid hydrolysis [29]. Waxy maize starch was dispersed in an aqueous solution of 3.16 mol/L sulphuric acid, the mass of the starch was 10% (w/v) of the volume of the sulphuric acid solution. The mixture was stirred continuously at a speed of 200 r/min at 40 °C for 6 days. After 6 days, the hydrolysed product was centrifuged and washed with water until the pH reached 6–8. At the end, the starch nanocrystals (SNC) were obtained by lyophilisation followed by grinding. As shown in Figure 1, the starch nanocrystal (SNC) samples were obtained after 6 days of sulphuric acid digestion hydrolysis of waxy maize starch and their electronic SEM and XRD images.

2.3 Sedimentary SNC
SNC in different mass percentages (0.1 wt%, 0.3 wt% and 0.5 wt%) of the basalt fibre composites were dispersed in anhydrous ethanol by ultrasonic treatment. Anhydrous ethanol and SNC were mixed in a ratio of 5:1 and the mixture was treated with ultrasound at a temperature of 35 °C and a frequency of 60 kHz. After dispersion, an equal amount of basalt fibres (0.5 wt%) was added to the SNC-alcohol suspension, and the mixture was stirred at a speed of 600 r/min. Following thorough mixing, the solution was transferred to a culture dish and placed in
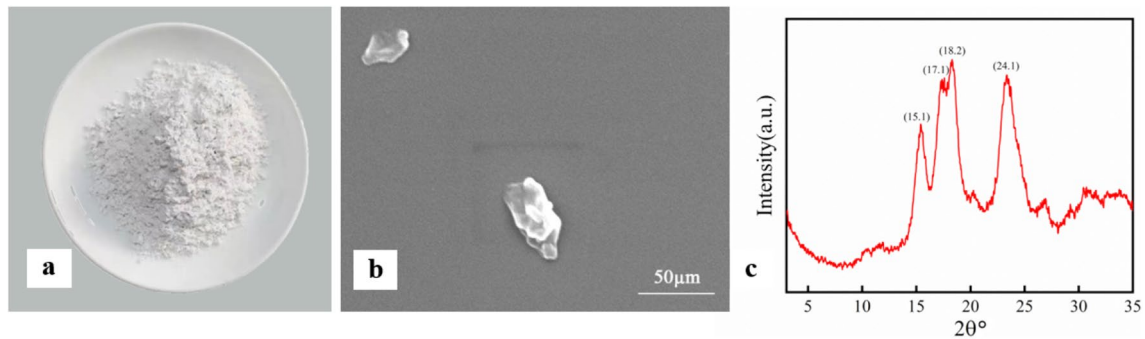
Figure 1 Starch nanocrystals and SEM/XRD images: (**a**) Sample of SNC, (**b**) SEM image of SNC, (**c**) XRD image of SNC

Table 1 Comparison of quality before and after drying of basalt fibre deposited SNC

SNC concentration (wt%)	0.1	0.3	0.5
Before the deposition (g)	0.65	0.86	1.08
After the deposition (g)	0.58	0.74	0.93

Table 2 SNC and CBF content of each specimen

Specimen number	SNC content (wt%)	Basalt fiber content (wt%)
BS-0	0	0
BS-1	0	0.5
BS-2	0.1	0.5
BS-3	0.3	0.5
BS-4	0.5	0.5

a vacuum drying oven set at a temperature of 40 °C for 40 h. After drying, the samples were removed, weighed, and the mass comparison before and after deposition was documented in Table 1.

2.4 Specimen Preparation

In order to strengthen the interface by various means, the current methods of preparation of fibre-reinforced composites are generally pressure processing, such as vacuum introduction, pressure tanks. For a more accurate analysis of the strengthening effect of nano-starch crystals on the interface, the influence of the process method on the interface needs to be excluded. Therefore, the method used in this experiment was compressionless forming.

Basalt fibres with different percentages of SNC were combined with epoxy resin at a stirring speed of 1000 r/min for 5 min. Epoxy hardener was then added for a second stirring phase at the same speed of 1000 r/min for 1 min. The homogenised mixture was then poured into a tensile mould to produce tensile specimens as described in Ref. [30]. These specimens were systematically labelled according to the categorisation in Table 2. The detailed specimen preparation procedure is shown in Figure 2.

2.5 Scanning Electron Microscopy (SEM)

After the tensile test, the microstructure of each specimen section was observed by scanning electron microscopy (Chech TESCAN, VEGA3). Before the scanning electron microscope observation, all specimen surfaces were gold sprayed with a vacuum evaporato (Japan JEOL

Corporation, JFC-1800) to improve the electrical conductivity of the specimen fracture surfaces.

2.6 FTIR Analysis

The samples were analysed using Fourier infrared spectroscopy (Japan Shimadzu Corporation, IRAffinity-1) to assess the compositional changes of the samples tested. FT-IR spectra of samples recorded in the range of 400–4000 cm^{-1} with a resolution of 2 cm^{-1}.

2.7 Mechanical Properties
2.7.1 Tensile Test

Tensile test using the universal testing machine (United States MTS Systems Corporation, WSM-10KN) at Key Laboratory of Bionics Engineering, Ministry of Education, Jilin University. The tensile strength, Young's modulus and elongation at break of the tensile specimens were determined by stretching the specimens at a loading rate of 1 mm/s [30]. Five replicate tests were carried out on each type of sample and the average of the five tests was taken as the sample test result. The force and displacement of the specimen during the test are recorded by load and displacement transducers. Based on the distruction surface of the specimen after each test, the cross-sectional dimensions of the samples are accurately calculated, the formula for calculating the tensile strength is as follows:
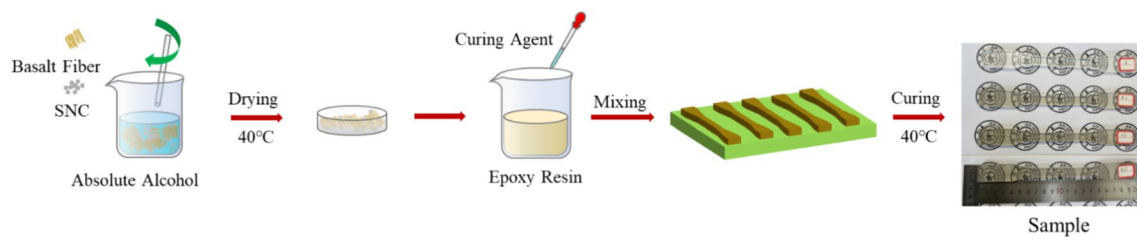
Figure 2 Schematic diagram of the test flow

$$\sigma = \frac{F_b}{S_0}, \qquad (1)$$

where σ is the tensile strength, F_b is the maximum tensile force at breakage of the sample, S_0 is the fracture area, the value of F_b can be obtained from the test data. Young's modulus was obtained from the slope of the stress-strain curve and elongation at break was obtained from experimental data.

3 Results and Discussion

3.1 Experimental Analysis of Mechanical Properties

The effect of different levels of SNC on the mechanical properties of basalt fibre composites was investigated by tensile tests. The picture of each specimen after stretching is shown in Figure 3(a). Three important performance indicators are examined in the tensile test, including tensile strength, Young's modulus and elongation at break. Figure 3(c) shows the tensile strength, Young's modulus and elongation at break of each specimen after the addition of different levels of SNC.

Tensile test results show that the tensile strength of the specimen decreases from 19.6 MPa to 14.7 MPa with the addition of SNC only. This indicates that instead of improving the mechanical properties of the resin, the addition of SNC created a large number of defects in the resin due to the lack of an effective interfacial bond. This results in the formation of a stress concentration within the specimen during tension, leading to a decrease in its tensile strength. As can also be seen in Figure 3(c), poor interfacial bonding also led to a reduction in the elongation at break of the samples. When 0.1 wt% SNC and 0.5 wt% CBF were added to the resin, the strength of the specimen increased by 13.6% to a value of 16.7 MPa. As the mass of SNC deposited on the CBF surface increases to 0.3 wt% and 0.5 wt%, the specimen strength also increases from 16.7 MPa to 19.75 MPa and 24.25 MPa. Owing to the deposition of SNC on the CBF surface via electrostatic effects, SNC is distributed within the composite at the interface. The observed enhancement in the composite's strength, attributable to the addition of SNC, signifies that SNC exerts a reinforcement/modification effect at the fiber/resin interface. Furthermore,

the increase in SNC content not only completely compensates for the defects formed at the interface in the composite, but also gives the basalt fibres a significant strengthening effect by reinforcing the interface.

The data on the tensile strength of the test specimens give the following main types of information. Firstly, the addition of small amounts of basalt fibres not only does not enhance the mechanical properties of the composite, but also reduces the tensile strength of the composite. Secondly, the tensile properties of the composites show an increasing trend with the addition of a small amount of SNC, but there is still a certain gap between the tensile properties of pure epoxy resin materials. When the SNC addition content becomes 0.3 wt%, the stress and strain values of the epoxy resin exceed the values associated with the pure epoxy resin material. This indicates that when the SNC content of the resin is increased, the mechanical properties of the material are improved. When the SNC addition content becomes 0.5 wt%, the highest tensile strength of the specimen can be seen in Figure 3(c).

At the meantime, with the increase in SNC content, the elongation at break of the composite recovered and surpassed that of the pure resin material. This indicates that there are no stress concentrations and local distortions due to defects arising from bad interfaces during the stretching process. As can be seen, the change in Young's modulus of each sample is not significant. This indicates that no new chemical substance is formed in each sample after the addition of SNC and that the chemical bonding of each sample does not change significantly.

3.2 SEM Analysis

Figure 3(d) shows the microstructure of the individual specimens at break in tension. As seen in Figure 3(d), the fracture of BS-0 is characterized by cleavage fracture, which is consistent with the brittle fracture of pure epoxy resin. With the addition of CBF, a large number of holes were visible in the section of specimen BS-1. These smooth holes are caused by the fibres pulling out of the resin matrix during the stretching process. This indicates that no effective interfacial bond was formed between the basalt fibers and the resin. This causes

Wei *et al. Chinese Journal of Mechanical Engineering*   (2024) 37:44

Page 5 of 8
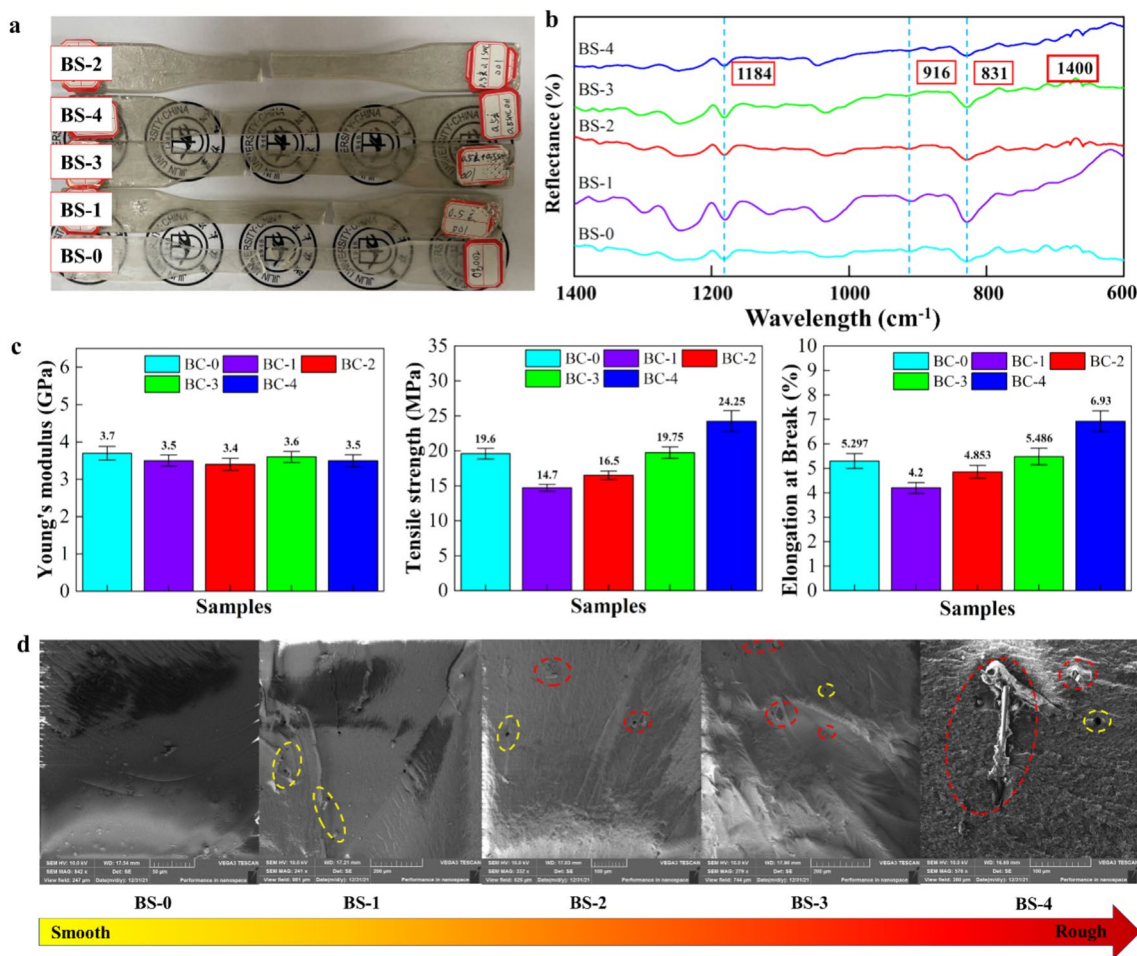
Figure 3 Tensile test results and interface characterization: (**a**) Picture of each specimen after stretching, (**b**) FT-IR spectra of each specimen, (**c**) Tensile strength, Young's modulus and elongation at break for each specimen, (**d**) SEM image of tensile fracture surface

stress concentrations to form at the interfacial junction of the composite during the tensile process, resulting in a reduction in the tensile strength and elongation of the composite. As seen on specimen BS-2, although the CBF with 0.1 wt% SNC deposited on the surface was also pulled out of the resin during stretching. However, basalt fibres that fracture in tandem with the epoxy have also emerged, with the epoxy resuming its rational fracture characteristics. This indicates that the interfacial bonding between CBF and epoxy resin was improved after depositing a small amount of SNC. During this period, the fracture reappears as a cleavage fracture feature, which indicates that the resin plays a major load-bearing role and the tensile strength of the specimen is recovered.

As seen on specimen BS-3, the number of holes in the composite cross-section decreased significantly with further increase in the SNC content deposited on the CBF surface, and simultaneous fracture of fibers

and resin was common. This indicates that the fibres start to play a load-bearing role during the stretching process, which is also consistent with the stretching results. It is worth noting that around some of the fibre fracture locations, the epoxy resin shows features of plastic deformation. This indicates that the addition of SNC has transformed the toughness of the epoxy resin around the basalt fibres. As the amount of SNC deposited increases, this effect becomes more pronounced in the SEM image of sample BS-4. This transformation not only shows that the deposition of SNC on the surface of basalt fibres significantly strengthens the interfacial bond between the fibres and the resin, but also effectively improves the coordination between the resin matrix and the fibres during load-bearing. This phenomenon is reflected in the mechanical properties of the specimen in the form of an increase in tensile strength and elongation at break.

Wei *et al. Chinese Journal of Mechanical Engineering*   (2024) 37:44

Page 6 of 8

3.3 FT-IR Analysis

Although tensile tests and SEM tests have shown that the addition of CBF with SNC attached helps to improve the interfacial bonding between the fibres and the resin in fibre-reinforced composites. In order to more precisely characterise the mechanism of action of the CBF addition, infrared spectroscopy tests were used to characterise the chemical reactions at the interface.

Figure 3(b) shows the infrared spectra of each specimen. 1184 cm^{-1}, 831 cm^{-1} and 916 cm^{-1} are the characteristic bands of the epoxy resin. It is clear from the graph that the intensity of the wave peak at 916 cm^{-1} of specimen BS-4 becomes significantly lower. This indicates that during the exothermic curing of the resin, the right amount of SNC causes crosslinking reaction between the resins and between the fibres. An excellent interfacial bonding is formed between the resin matrix and the basalt fibres, allowing the curing reaction of epoxy resin more fully in response. At the meantime, the strength of the non hydroxy-terminated –OH stretching vibration is enhanced, generating a reticulate homopolymer containing an ether bond C–O–C structure, promotes the formation of a three-dimensional cross-linked net-like structure within the epoxy resin system. This further explains the significant increase in tensile strength of BS-4 specimens containing 0.5 wt% CBF, 0.5 wt% SNC.

The results of the infrared spectra corroborate the previous analysis. When using the non-pressure forming method, as shown in Figure 4(a), the smooth basalt fibre surface does not form a good interfacial bonding with the epoxy resin. The epoxy resin surrounding the basalt fibres forms a hole with a smooth inner wall, this hole forms a stress concentration when stretched. This leads to rapid crack expansion between the holes and reduces the

mechanical properties of the composite. As shown in Figure 4(b), CBF with SNC deposited on the surface reacts chemically with the epoxy resin during the curing process, resulting in a homopolymer with an ether bonded C–O–C structure in the form of a network. This allows the CBF to be force-constrained, exerting a load-bearing role during tension, and also avoiding the appearance of holes and stress concentrations. The addition of SNC enhances the interfacial bond between the epoxy resin and the CBF, enabling the CBF to achieve an effective load-bearing effect and improving the mechanical properties of the composite.

4 Conclusions

The approach outlined in this paper, involving the reinforcement of basalt fibre-epoxy resin composites with starch nanocrystals, offers significant potential for the use of starch nanocrystals derived from agricultural crops in the field of composite materials. The following conclusions can be obtained from this paper:

(1) Under compressionless forming conditions, the addition of basalt fibres alone does not strengthen the epoxy resin, but rather reduces the strength of the composite.

(2) With the addition of SNC deposited on the surface of the basalt fibres, the tensile strength of the composite is restored and gradually becomes higher than that of the resin matrix. When SNC was added at 0.5 wt%, the tensile strength of the composite increased by 23.7% compared to the sample without the addition of SNC.

(3) Microstructural analysis shows that the basalt fibres alone do not play a reinforcing role in the com-
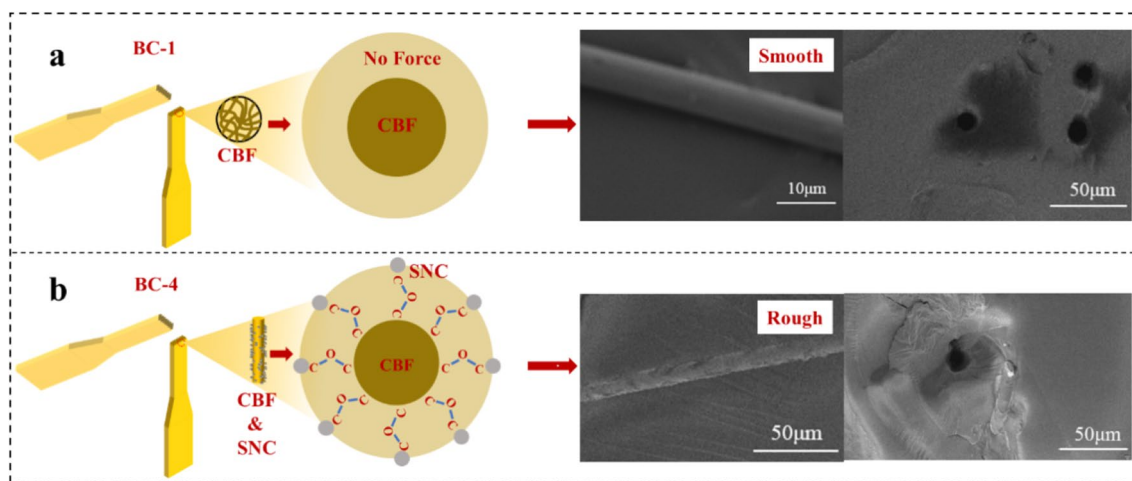
Figure 4 Schematic of the mechanical properties of SNC reinforced composites

posite because no effective interfacial bonding is formed during the pressure-free forming process.

(4) During the stretching process, smooth holes form on the fracture surface due to the pull-out of the basalt fibres. The smooth holes create stress concentrations that reduce the mechanical properties of the composite.

(5) As the SNC content deposited on the CBF surface increases, simultaneous fracture of the CBF and the epoxy resin begins to occur. This is due to the addition of SNC facilitating the curing reaction of the epoxy resin, resulting in an increase in the strength of the stretching vibrations of the non hydroxy-terminated –OH and the formation of a homopolymer with an ether bond C–O–C structure in a network. This enhances the interfacial bond between the fibres and the matrix, allowing the fibres to perform an excellent mechanical load-bearing role and increasing the strength of the composite.

Declarations

Competing Interests
The authors declare no competing financial interests.

References

[1] V Fiore, T Scalici, G D Bella, et al. A review on basalt fibre and its composites. *Composites Part B-Engineering*, 2015, 74: 74–94.

[2] G Wu, X Wang, Z S Wu, et al. Durability of basalt fibers and composites in corrosive environments. *Journal of Composite Materials*, 2015, 47(7): 873–887.

[3] B Z Sun, Z L Niu, L T Zhu, et al. Mechanical behaviors of 2D and 3D basalt fiber woven composites under various strain rates. *Journal of Composite Materials*, 2010, 44(14): 1779–1795.

[4] R Liu, W Cao, T X Fan, et al. Development of processing maps for 3 vol.% TiCp/AZ91D composites material. *Materials Science and Engineering A-Structural Materials Properties Microstructure and Processing*. 2010, 527(18-19): 4687–4693.

[5] A Abdi, R Eslami-Farsani, H Khosravi. Evaluating the mechanical behavior of basalt fibers/epoxy composites containing surface-modified $CaCO_3$ nanoparticles. *Fibers and Polymers*, 2018, 19(3): 635–640.

[6] Y H kim, D H Yang, S W Yoon, et al. A study on the mechanical properties comparison for the composites application of basalt fibers with GFRP. *Advanced Science Letters*, 2011, 4(4-5): 1633–1637.

[7] S Zhandarov, E Mader. Characterization of fiber/matrix interface strength: applicability of different tests, approaches and parameters. *Composites Science and Technology*, 2005, 65(1): 149–160.

[8] M C Seghini, F Touchard, F Sarasini, et al. Engineering the interfacial adhesion in basalt/epoxy composites by plasma polymerization. *Composites Part A-Applied Science and Manufacturing*, 2019, 122: 67–76.

[9] B C Ray, D Rathore. Durability and integrity studies of environmentally conditioned interfaces in fibrous polymeric composites: Critical concepts and comments. *Advance in Colloid and Interface Science.* 2014, 209: 68–83.

[10] S R White, M M Caruso, J S Moore. Autonomic healing of polymers. *Mrs Bulletin*, 2008, 33(8): 766–769.

[11] J J Wang, S F Zhou, J Huang, et al. Interfacial modification of basalt fiber filling composites with graphene oxide and polydopamine for enhanced mechanical and tribological properties. *RSC Advances*, 2018, 8(22): 12222–12231.

[12] C Scheffer, T Forster, E Mader, et al. Aging of alkali-resistant glass and basalt fibers in alkaline solutions: Evaluation of the failure stress by Weibull distribution function. *Journal of Non-Crystalline Solids*, 2009, 335(52-54): 2588–2595.

[13] Z Li, L Xiao, Q Y Pan, et al. Corrosion behaviour and mechanism of basalt fibres in acidic and alkaline environments. *Corrosion Science*, 2016, 110: 15–22.

[14] M S Islam, Y Deng, L Y Tong, et al. Grafting carbon nanotubes directly onto carbon fibers for superior mechanical stability: Towards next generation aerospace composites and energy storage applications. *Carbon*, 2016, 96: 701–710.

[15] N Preda, A Costas, M Lilli, et al. Functionalization of basalt fibers with ZnO nanostructures by electroless deposition for improving the interfacial adhesion of basalt fibers/epoxy resin composites. *Composites Part A-Applied Science and Manufacturing*, 2021, 149: 106488.

[16] K Mylsamy, I Rajendran. Influence of alkali treatment and fibre length on mechanical properties of short agave fibre reinforced epoxy composites. *Materials & Design*, 2011, 32(8-9): 4629–4640.

[17] M S Sreekala, M G Kumaran, S Joseph. Oil palm fibre reinforced phenol formaldehyde composites: Influence of fibre surface modifications on the mechanical performance. *Applied Composite Materials*, 2000, 7(5–6): 295–329.

[18] B Wei, S H Song, H L Cao, et al. Strengthening of basalt fibers with nano-SiO2-epoxy composite coating. *Materials & Design*, 32(8-9): 4180–4186.

[19] F P La Mantia, M Morreale. Green composites: A brief review. *Composites Part A-Applied Science and Manufacturing*, 2011, 42(6): 579–588.

[20] A Kaushik, R Kaur. Thermoplastic starch nanocomposites reinforced with cellulose nanocrystals: Effect of plasticizer on properties. *Composite Interfaces*, 2016, 23(7): 701–717.

[21] S George, S Pokhrel, T Xia, et al. Use of a rapid cytotoxicity screening approach to engineer a safer zinc oxide nanoparticle through iron doping. *ACS Nano*, 2010, 4(1): 15–29.

[22] Nechyporchuk, M N Belgacem, J Bras. Production of cellulose nanofibrils: A review of recent advances. *Industial Crops and Products*, 2016, 93(2–25): SI.

[23] X Z Xu, F Liu, L Jiang, et al. Cellulose nanocrystals vs. cellulose nanofibrils: A comparative study on their microstructures and effects as polymer reinforcing agents. *ACS Applied Materials & Interfaces*, 2013, 5(8): 2999–3009.

[24] Z S Zhang, Y Li, C Z Chen. Synergic effects of cellulose nanocrystals and alkali on the mechanical properties of sisal fibers and their bonding properties with epoxy. *Composites Part A-Applied Science and Manufacturing*, 2017, 101: 480–489.

[25] A H Pei, J M Malho, J Ruokolainen, et al. Strong nanocomposite reinforcement effects in polyurethane elastomer with low volume fraction of cellulose nanocrystals. *Macromolecules*, 2011, 44(11): 4422–4427.

Wei *et al. Chinese Journal of Mechanical Engineering*   (2024) 37:44

Page 8 of 8

[26] H Angellier, S Molina-Boisseau, P Dole, et al. Thermoplastic starch-waxy maize starch nanocrystals nanocomposites. *Biomacromolecules*, 2006, 7(2): 531–539.

[27] N L Garcia, L Ribba, A Dufresne, et al. Effect of glycerol on the morphology of nanocomposites made from thermoplastic starch and starch nanocrystals. *Carbohydrate Polymers*, 2011, 1: 203–210.

[28] H Zheng, F J Ai, P R Chang et al. Structure and properties of starch nanocrystal-reinforced soy protein plastics. *Polymer Composites*, 2009, 30(4): 474–480.

[29] J Zhou, J Tong, X G Su, et al. Hydrophobic starch nanocrystals preparations through crosslinking modification using citric acid. *International Journal of Biological Macromolecules*, 2016, 91: 1186–1193.

[30] State Administration for market regulation, Inspection and Quarantine of the People's Republic of China; GB/T 2567-2021 Test methods for properties of resin casting body. **(in Chinese)**

Yanpeng Wei   born in 1998, is currently a postgraduate student at *College of Biological and Agricultural Engineering, Jilin University, China.*

Jiale Zhao   born in 1986, is currently a professor at *Key Laboratory of Bionics Engineering, Ministry of Education, Jilin University*. He received his PhD degree from *Jilin University, China*. His research interest includes Intelligent bionic machinery.

Jian Zhuang   born in 1981, is currently a professor at *College of Biological and Agricultural Engineering, Jilin University, China.* He received his PhD degree from *Jilin University, China*. His research interest includes biomimetic composite material.

Peng Zhang   born in 1971, is currently a professor at *Weichai Lovol Heavy Industry Co., LTD, China.*

Zhiwu Han   born in 1969, is currently a professor at *Key Laboratory of Bionics Engineering, Ministry of Education, Jilin University, China*. He received his PhD degree from *Yanshan University*. His research interest includes biomimetic mechanical system.